Effective Extraction and Filtering of Frequency Components in Physiological Signals Using Sum-of-Sinusoids Modelling

José L. Ferreira[*1], Ronald M. Aarts[2], Pierre J. M. Cluitmans[3]

[1,2,3]Department of Electrical Engineering, Eindhoven University of Technology
[2]Philips Research Laboratories Eindhoven
[3]Kempenhaeghe Epilepsy Center
P. O. 513 – 5600 MB – Eindhoven – The Netherlands

[*1]j.l.ferreira@tue.nl; [2]r.m.aarts@tue.nl; [3]p.j.m.cluitmans@tue.nl

Abstract

In biological signal processing, modelling and extraction of specific frequency components constitute an important procedure for filtering signal components of interest as well as artefact removal. Under some interference scenarios, a satisfactory elimination of artefacts from the signal must be even performed by subtraction of an artefact waveform model or template, rather than the use of linear band-pass filters. That is the case of the gradient artefact induced in the EEG within the fMRI scanner, which cannot be characterized by a specific bandwidth or spectral content. This paper presents a simple and accurate approach based upon sum-of-sinusoids modelling for signal and artefact frequency components representation in physiological signals. According to the proposed method, each signal frequency component is approximated as a sinusoid, whose amplitude and phase parameters are estimated by making use of the Discrete Fourier Transform (DFT). The proposed approach reveals to perform an effective modelling and extraction of ECG signal components as well as underlying gradient artefacts in the EEG signal.

Keywords

Biological Signal Modelling; Sum-of-Sinusoids Modelling; Gradient Artefact Correction; Biological Signal Filtering

Introduction

Filtering and extraction of signal frequency components are ubiquitous and essential practices in biological and digital signal processing in general. The usage of filtering methodologies allows removal of undesirable noise components, artefacts, and other types of interference, which is fundamental for obtaining an enhanced signal. In the same way, filtering approaches allow extraction of frequency components and bandwidths of interest (Oppenheim, 1999; Proakis and Manolakis, 1996; Rangayyan, 2002).

Filtering of signal components is commonly performed by linear digital filters. Digital filtering techniques are also termed "frequency-selective filters", and can be implemented in time and frequency-domain. Ideally, a filter is a linear-time invariant system that passes certain frequency components, and all others located outside the filter cut-off frequency are rejected. In practice, real filters do not achieve complete removal of frequencies outside the filter cut-off frequency. A transition region occurs around the cut-off frequency in such a way that the magnitude response is not constant in the entire filter pass-band as well (Oppenheim, 1999; Proakis and Manolakis, 1996).Furthermore, concerning removal of physiological and some other types of interference, linear band-pass filters could not be effective since the former cannot be characterized by any specific spectral content or frequency bandwidth (Rangayyan, 2002; Allen et al., 1998; Allen et al., 2000).

In such cases, the usage of non-linear filtering approaches for modelling noise components constitutes an alternative method for filtering and extraction of signal components, like the subtraction in time and frequency-domain methodologies. According to the subtraction in time-domain approach, when the noise or artefact can be assumed to possess a stationary waveform (i.e., it can be considered a slowly varying process), an average waveform or template which represents the artefact can be estimated. Then, such a template is subtracted from the signal to achieve the signal restoration (Allen et al., 1998; Allen et al., 2000). The same procedure can be performed in frequency-domain when it is possible to assume that the noise power spectrum does not change significantly in-between the update periods (Vaseghi, 2000).

In this way, Allen et al. (2000) proposed the usage of an average artefact waveform in order to represent and remove the gradient artefact. Such an artefact is induced in the EEG signal by varying gradient magnetic fields within the fMRI scanner. The frequency components of the gradient artefact cannot be cleaned up simply by applying usual low-pass filtering because of the underlying frequency-components which remains in the clinical EEG bandwidth (Niazy et al., 2005). Hence, their removal requires the usage of other filtering techniques, rather than low-pass filters (Allen et al., 2000). Instead of using an average template, El-Tatar and Fokapu (2011) and Ferreira et al. (2013) proposed the usage of an artefact waveform estimate based upon a set of sinusoidal waveforms, for implementation of the gradient artefact modelling and subsequent EEG restoration. In addition to estimating the artefact waveform, the sum-of-sinusoids model can be used to predict the variability of the gradient artefact waveform over the time (Ferreira et al., 2013).

The sum of sinusoids is widely employed for representation and analysis/synthesis of speech and audio signals, which reassumed as periodic signals. Such a signal representation has proven to be effective because of its widespread applicability and simplicity of implementation (Brillinger, 1987; Prasad et al., 2008; McAulay and Quatieri, 1986). This paper presents a simple and accurate approach for modelling of signal frequency components of interest and artefacts in physiological signals by the sum of a set of sinusoids. Our method constitutes a modification from the approach proposed by Ferreira et al. (2013) for removal of underlying gradient artefacts from the EEG signal bandwidth. According to our methodology, each signal frequency component is approximated separately as a sinusoid, whose amplitude parameter is estimated by using the magnitude of the Discrete Fourier Transform (DFT). The phase of the DFT is used for estimation of the sinusoid phase as well, as described in the section Methods. The proposed method shows to perform an effective modelling of ECG signal components as well as a satisfactory removal of underlying gradient artefacts from the EEG signal by the subtraction of the estimated sum-of-sinusoids model, as shown in the section Results.

Methods

Signal Frequency Components Modelling

The Discrete Fourier Transform (DFT) can be used to decompose a finite a periodic discrete-time sequence, y_i, into its k complex sinusoids or exponential components. In the opposite way, the Inverse Discrete Fourier Transform (IDFT) allows recovering y_i from those resulting components. In the literature, some approaches have been described in order to compute the DFT and the IDFT efficiently, known collectively as Fast Fourier Transform (FFT) algorithms (Proakis and Manolakis, 1996).Eqs. (1) and (2) constitute one representation of such FFT algorithms (Oppenheim, 1999):

$$Y_k = \sum_{i=1}^{N} y_i \omega_N{}^{(i-1)(k-1)}, \quad (1)$$

$$y_i = \frac{1}{N}\sum_{k=1}^{N} Y_k \omega_N{}^{-(i-1)(k-1)}, \quad (2)$$

where Y_k is the Discrete Fourier Transform of y_i; N is the length of y_i; and $\omega_N = e^{-j2\pi/N}$.

Each frequency component of y_i can be also fitted or approximated by the following sinusoid waveform (Brillinger, 1987; Ferreira et al., 2013):

$$\hat{s}_{k,i} = \hat{A}_k \cos\left(2\pi f_k t_i + \hat{\phi}_k\right), \quad (3)$$

where the amplitude $\hat{A}_k$ is estimated by using the DFT magnitude of the *k-th* frequency component and the signal length associated with y_i:

$$\hat{A}_K = \frac{2 \times |Y_k|}{N}. \quad (4)$$

The time t_i is computed as:

$$t_i = i\Delta t, \quad (5)$$

where Δt corresponds to the inverse of the sampling frequency f_s. The frequency f_k, assumed known, is provided by Eq. (6):

$$f_k = k\frac{f_s}{N}. \quad (6)$$

In order to match f_k with the corresponding frequency component within y_i, N was set as a multiple of the ratio f_s / f_k.

Estimation of the sinusoidal phase is performed by calculating the DFT phase of the *k-th* frequency component:

$$\hat{\phi}_k = \arctan\left[\frac{\Im(Y_k)}{\Re(Y_k)}\right]. \quad (7)$$

Consistency Analysis

Our methodology was implemented in MATLAB environment. For analysis of consistency, Eqs. (1) – (7) were applied for estimating a single sinusoid (s_i) in Gaussian white noise (n_i):

$$y_i = s_i + n_i. \quad (8)$$

Zero mean Gaussian white noise was mixed with

single sinusoids possessing different frequencies f_k (0.25, 3, 10, 50, 200, and 800 Hz).The SNR of the resulting (observed) signal was varied from -10 to 60 dB. At each SNR, 100 trials were carried out in order to estimate the percent error for the sinusoid amplitude and phase estimates $(\hat{\theta}_k)$:

$$error = 100 \times \frac{\bar{\hat{\theta}}_{k,q} - \theta_k}{\theta_k}\%, \quad (9)$$

where $\bar{\hat{\theta}}_{k,q}$ is the average of the parameter estimate, taking into account the 100 performed trials. Also the mean square error (MSE), ϱ_{MSE}, characteristics were estimated by Eq. (10):

$$\varrho_{MSE} = -10 \times \log\left[\frac{1}{100}\sum_{q=1}^{100}\left(\hat{\theta}_{k,q} - \theta_k\right)^2\right], \quad (10)$$

In order to assess the performance of the sinusoidal phase and amplitude estimation, the Cramer-Rao Bound (CRB) was also calculated using Eqs. (11) and (12) (Proakis and Manolakis, 1996; Papoulis and Pillai, 2002; Kay, 1993):

$$\text{var}(\hat{A}_k) \geq \frac{2 \times \sigma^2}{N}, \quad (11)$$

$$\text{var}(\hat{\phi}_k) \geq \frac{2 \times \sigma^2}{N \times A_k^2}, \quad (12)$$

where σ^2 corresponds to the variance of the Gaussian noise.

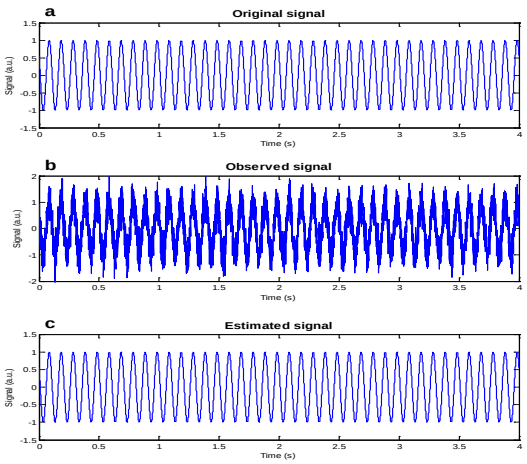

FIG. 1 APPLICATION OF EQS. (1) – (7) FOR ESTIMATING A SINGLE SINUSOID MIXED WITH WHITE GAUSSIAN NOISE: (A) ORIGINAL SINUSOID (A_k = 1; ϕ_k = 1 rad); (B) OBSERVED (MIXED) SIGNAL (SNR = 10 dB); (C) ESTIMATED SINUSOID ($\hat{A}_k$ = 0.9995 a.u. AND $\hat{\phi}_k$ = 1.0004 rad)

Fig. 1b shows the single sinusoid of Fig. 1a (A_k = 1 a.u.; f_k = 10 Hz; ϕ_k = 1 rad; N = 8192) mixed with Gaussian white noise, SNR = 10 dB. Δt was set at 1/2048 Hz. In Fig. 1c, the sinusoid estimated by using the approach of Eqs. (1) – (7) is depicted. The corresponding percent error is equal to -0.0492% and 0.0440%, respectively, for $\hat{A}_k$ and $\hat{\phi}_k$. In Table 1, the percent error for different values of frequency f_k is shown, considering different SNR levels and a sinusoid length N = 8192. It can be observed that as the SNR increases, the estimated error for the amplitude and phase estimation tends to 0%.

TABLE 1 ESTIMATED PERCENT ERROR ACCORDING TO EQ. (9), FOR DIFFERENT VALUES OF FREQUENCY f_k, SNR, AND 100 TRIALS

SNR (dB)	θ_k	Percent error (%)				
		f_k(Hz)				
		3	**10**	**50**	**200**	**800**
-10	A_k	0.0124	0.3952	-0.1403	0.4761	0.3278
	ϕ_k	-0.3264	-0.5420	0.1501	0.4713	-0.1010
0	A_k	-0.3625	-0.0162	-0.0023	-0.1481	-0.0675
	ϕ_k	-0.1338	-0.0043	0.0085	0.2510	-0.0541
10	A_k	-0.0569	-0.0313	-0.0157	0.0734	0.0570
	ϕ_k	-0.0213	0.0482	0.0308	-0.1029	-0.0522
20	A_k	0.0201	0.0226	0.0154	-0.0030	-0.0214
	ϕ_k	-0.0112	-0.0105	0.0012	0.0214	0.0011
30	A_k	0.0108	-0.0051	-0.0024	-9.7×10^{-4}	5.2×10^{-4}
	ϕ_k	-0.0045	1.9×10^{-4}	-0.0064	0.0093	-0.0030
40	A_k	0.0021	6.0×10^{-5}	3.6×10^{-5}	-0.0020	9.5×10^{-4}
	ϕ_k	0.0023	0.0017	-4.5×10^{-4}	-3.6×10^{-4}	-3.3×10^{-5}
50	A_k	6.1×10^{-4}	1.0×10^{-4}	-3.6×10^{-4}	9.4×10^{-4}	1.9×10^{-4}
	ϕ_k	-6.8×10^{-4}	-2.2×10^{-4}	-1.0×10^{-4}	-5.2×10^{-4}	-6.4×10^{-4}
60	A_k	-4.6×10^{-5}	-4.3×10^{-5}	2.0×10^{-5}	-2.5×10^{-4}	-1.2×10^{-4}
	ϕ_k	-5.1×10^{-5}	1.6×10^{-4}	-8.2×10^{-5}	2.2×10^{-4}	-2.5×10^{-5}

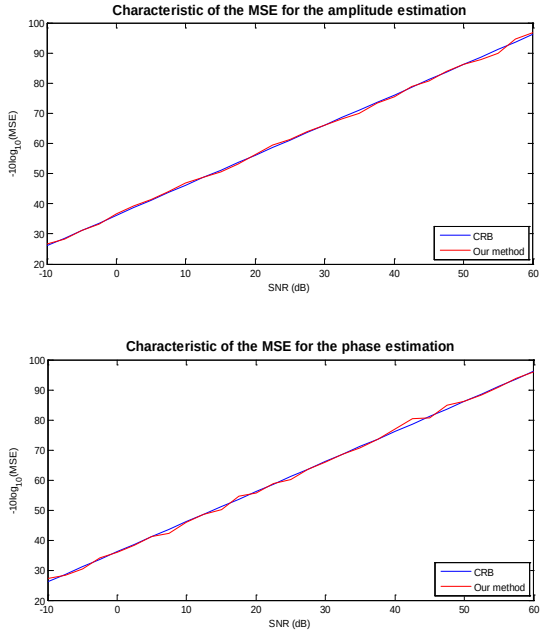

FIG. 2 CHARACTERISTICS OF THE MSE FOR THE AMPLITUDE AND PHASE ESTIMATIONS (N = 8192; f_k = 0.25 Hz; 100 TRIALS). SUCH CHARACTERISTIS ATTAIN THE CRB EVEN UNDER LOW SNR, DEMONSTRATING THE ACCURACY ESTIMATION OF THE PROPOSED MODELLING APPROCH

Fig. 2 depicts the MSE characteristics for the amplitude and phase parameters. It can be noticed that those characteristics closely attain the respective CRB estimates, even under low SNR. Also, the frequency

dependency for amplitude and phase estimations can be neglected (Table 1). Such characteristics, associated with the low percent error for the amplitude and phase parameters, show the accuracy of using Eqs. (1) – (7) for modelling and extraction of single sinusoidal frequency components (Kay, 1993). Therefore, they do indicate the feasibility of using the proposed method as a filter bank approach for modelling and extraction of signal frequency components (Goodwin, 2008; McAulay and Quatieri, 1986). Thus, we have applied Eqs. (1) – (7) for modelling larger bandwidths of real ECG excerpts as well as arising gradient artefacts in EEG signals. Such signals were collected for a research focused on epilepsy and post-traumatic stress disorder (Van Liempt et al., 2011; Ferreira et al., 2013).

The ECG/EEG (*EpG*) frequency components of interest were modelled as a sum of sinusoid components, as follows (Ferreira et al., 2013):

$$EpG_i = \sum_{k=1}^{K} \hat{s}_{k,i}, \quad (13)$$

Different values of signal length, N, were chosen in order to evaluate the influence of the signal length over the obtained results. The influence of the total number of K modelled frequency components was analysed during the methodology application as well.

Results

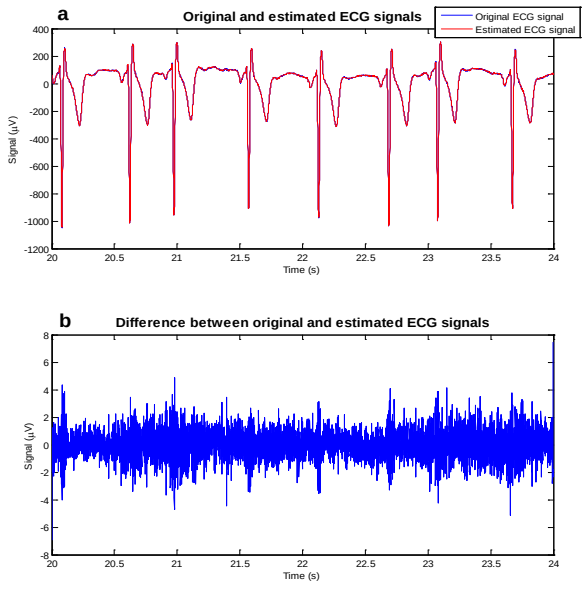

FIG. 3 (A) APPLICATION OF EQS. (1) – (7) FOR MODELLING THE FREQUENCY COMPONENTS OF AN ECG EXCERPT AND THE RESPECTIVE ESTIMATED SIGNAL. K = 1000 MODELLED FREQUENCY COMPONENTS OR SINUSOIDS (f_k RANGING FROM 0 TO 250 Hz) WERE TAKEN INTO ACCOUNT; (B) DIFFERENCE BETWEEN ORIGINAL AND ESTIMATED SIGNAL

Fig. 3 illustrates application of Eqs. (1) – (7) for modelling and extraction of frequency components in the ECG signal. In Fig. 3a, an exemplary ECG excerpt (original ECG signal: N = 8192; f_s = 2048 Hz) and the respective modelled signal resulting from the sum of a total K = 1000 sinusoid components (estimated ECG signal) are depicted. The value K = 1000 was calculated using Eq. (6), for f_k ranging from 0 to 250 Hz (f_K = 250 Hz), in accordance with the clinical frequency range of the electrocardiogram (Olson, 2010).

Clearly, it can be observed that the proposed approach effectively achieves to model the considered ECG bandwidth. For the signals of Fig. 3a, the cross-correlation coefficient is equal to 0.999. The difference between the original and estimated ECG depicted in Fig. 3b, therefore, corresponds to the non-modelled high-frequency activity above 250 Hz. Also it is noticed that increasing the number of K modelled components, the MSE decreases (Fig. 4a). The same behaviour is noted when N is increased, considering a specific f_K (Fig. 4b). In this case, however, the MSE stabilizes around a certain value (6 μV²) after the length of the signal reaches a certain number of samples, as expected.

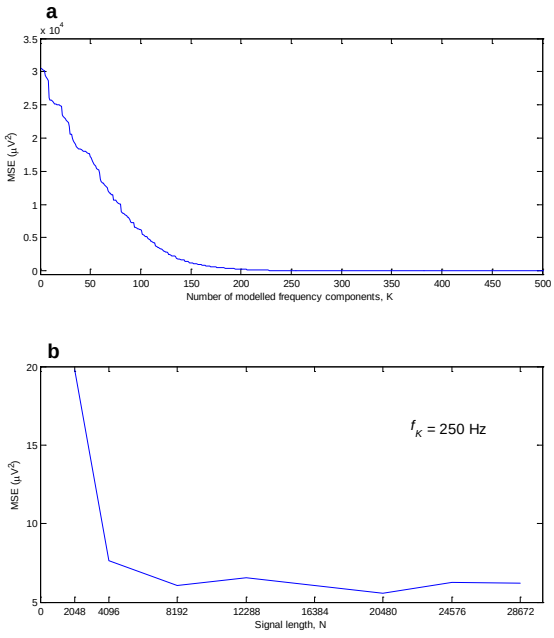

FIG. 4 MSE VARIATION FOR DIFFERENT VALUES OF: (A) k (RANGING FROM 1 TO 500; N = 8192); AND (B) N (f_K = 250 Hz)

Figs. 5 and 6 depict the usage of the proposed method for carrying out the gradient artefact waveform modelling and subsequent removal from the EEG signal, in accordance with Ferreira et al. (2013). Fig. 5a depicts four representative EEG excerpts (N = 4960; f_s =

2048 Hz), electrode positions P3, CP1, FC5, and F6 with gradient artefact interference (average around 1500 μVpk-pk), recorded from three different subjects In Fig. 5b, the respective low-pass filtered signals are depicted. As can be observed, considerable signal distortion is still observed in these signals because of the underlying artefact interference (Niazy et al., 2005).

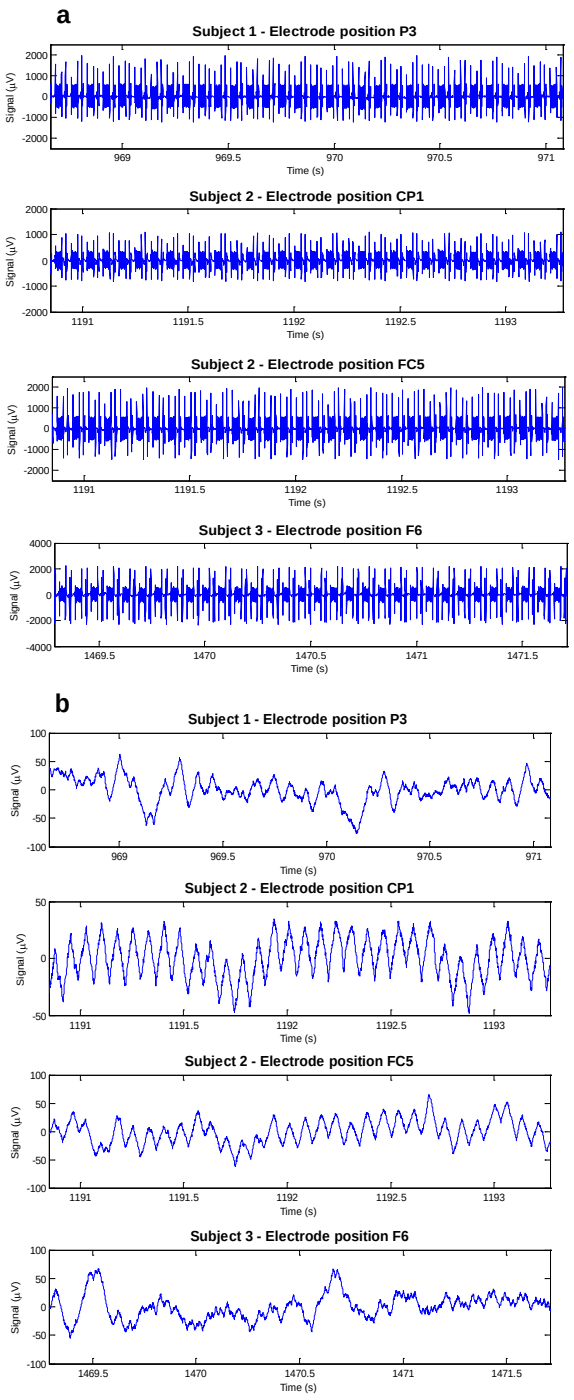

FIG. 5 (A) EEG EXCERPTS WITH GRADIENT ARTEFACT INTERFERENCE; (B) EEG SIGNALS OF (A) AFTER APPLICATION OF A LOW-PASS FILTER: A CONSIDERABLE DISTORTION IS STILL OBSERVED IN SUCH SIGNALS BECAUSE THE UNDERLYING ARTEFACT COMPONENTS WHICH REMAIN IN THE EEG BANDWIDTH

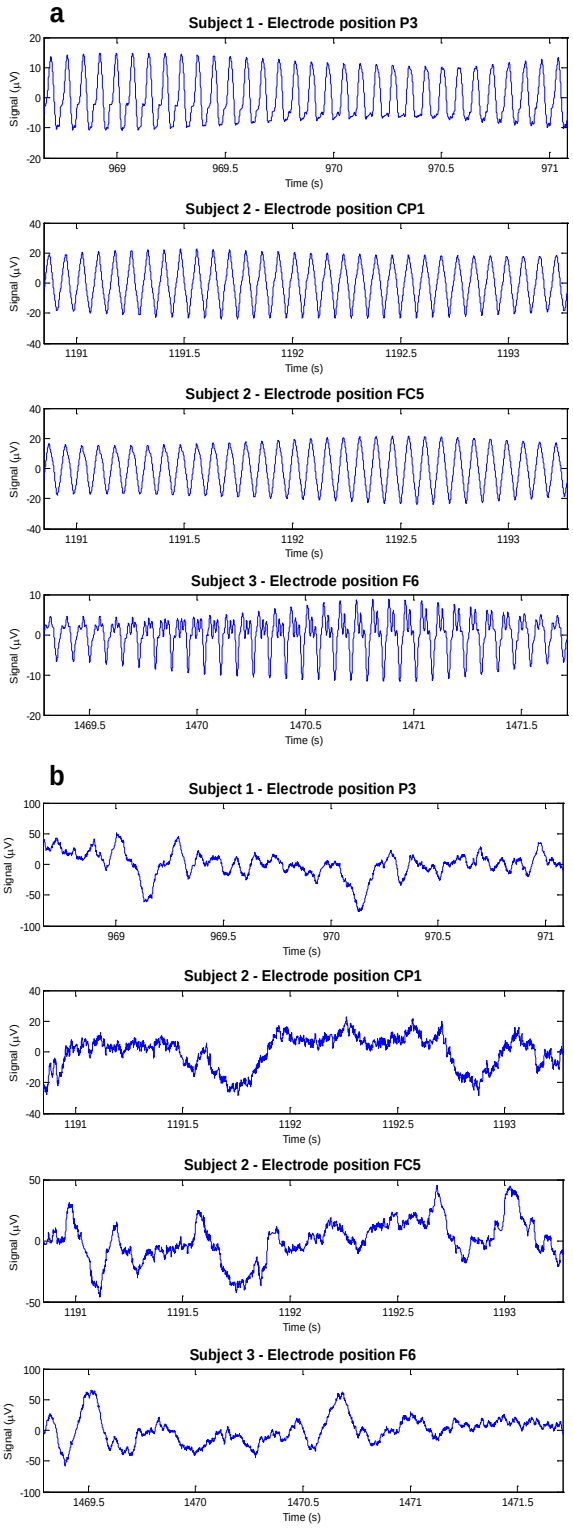

FIG. 6 (A) MODELLED UNDERLYING GRADIENT ARTEFACT OF THE SIGNALS OF FIG. 5B USING THE PROPOSED METHOD; (B) RESTORED EEG SIGNALS AFTER SUBTRACTION OF THE ARTEFACT WAVEFORM MODELS OF (A) FROM THE SIGNALS OF FIG. 5B

Hence, we used Eqs. (1) – (7) and (13) to model and subtract the frequency components corresponding to the underlying artefacts. According to Niazy et al. (2005), these frequency components occurs in

frequency bins, whose fundamental are multiples of the inverse of the echo-planar imaging slice time (ST). Thus, Eq. (6) is changed to:

$$f_k = k\frac{f_s}{ST}, \tag{14}$$

and the frequency components which arise into the region of ±1 Hz around the fundamental frequency were then modelled (Ferreira et al., 2013; Niazy et al., 2005).

Fig. 6a shows the resulting modelled underlying artefact for the EEG excerpts of Fig. 5b. In turn, Fig. 6b depicts the restored EEG after subtraction of the sum-of-sinusoids models of Fig. 6a from the signals of Fig. 5b. Finally, in Fig. 7, the waveforms obtained by averaging the artefact waveforms shown in Fig. 6a (segmented at each slice time), and estimated by the artefact average subtraction (AAS) method (Allen et al., 2000) are depicted for comparison purposes. The respective slice time taken into account for averaging is equal to 75.68 ms (= 155 samples)(Ferreira et al., 2012). The average cross-correlation calculated for these waveforms is equal to 0.996, considering all analysed EEG excerpts (Ferreira et al., 2013).

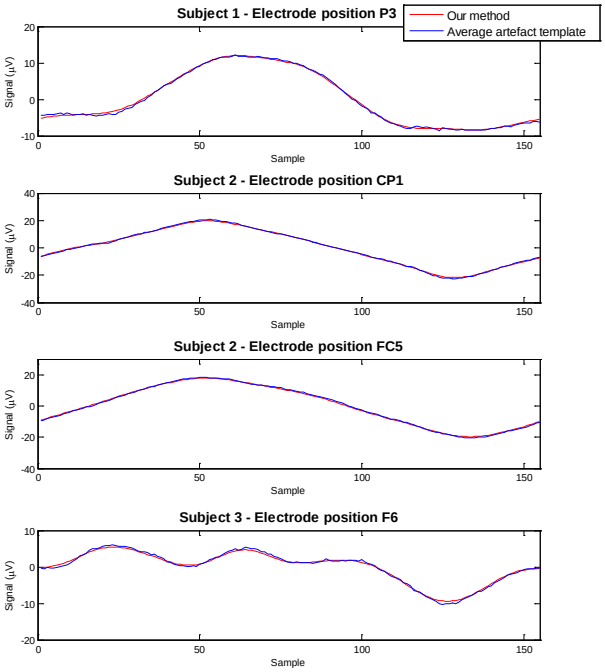

FIG. 7 AVERAGE ARTEFACT WAVEFORMS OBTAINED BY AVERAGING THE WAVEFORMS DEPICTED IN FIG. 6A (RED TRACE), AND OBTAINED BY THE AAS METHOD (BLUE TRACE). THESE WAVEFORMS ARE QUITE SIMILAR, SHOWING THAT THE ARTEFACT VARIABILITY OVER THE TIME IS PREDICTED BY THE SUM-OF-SINUSOID MODELS DEPICTED IN FIG. 6A

As can be observed in Figs. 6a and 7, the proposed method predicts the variability of the artefact waveform over the time, unlike the average template estimated by using the AAS method (Ferreira et al., 2013; Allen et al., 2000). This characteristic could be useful for investigating and understanding the nature and morphology of such interference as well as estimating a more accurate artefact waveform or template, in order to improve the EEG restoration (Ferreira et al., 2013; Allen et al., 2000; Koskinen and Vartiainen, 2009). As still observed by Ferreira et al. (2013), increasing of the length of the EEG excerpt results in approximating the artefact waveform represented by the sum-of-sinusoids model to the average waveform template estimated by the AAS method.

Discussion

As discussed by Brillinger (1987) and Prasad et al. (2008), the sum-of-sinusoids model can be used to provide some very important solutions and real life applications in different areas. For instance, in audio and speech processing, modelling based upon the sum of sinusoids has been widely employed because of its simplicity and flexibility of implementation (Goodwin, 2008; El-Tatar & Fokapu, 2011). In this way, by combining sum-of-sinusoids modelling with Discrete Fourier Transform properties, we have made use of the approach described in Eqs. (1) – (7) to obtain an analytical representation of frequency components in physiological signals.

As can be observed in Figs. 3, 6, and 7, frequency components of the ECG and gradient artefacts in EEG excerpts can be accurately modelled using the proposed methodology. For the ECG signals shown in Fig. 3a, the cross-correlation between the original and estimated signals is equal to 0.999 (average equal to 0.996), indicating strong frequency activity for the modelled bandwidth (0 – 250 Hz). Figs. 3b and 4 confirm these results. As depicted in Fig. 4, a low MSE is observed between original and estimated signals (at 6 μV^2), for a signal length higher than 8192 samples.

In the same way, as shown in Figs. 5, 6, and 7, the proposed approach achieves an accurate representation of the underlying gradient artefact waveform (Ferreira et al., 2013). Thereby, such an artefact can be satisfactorily removed from the EEG signal (Fig. 6b). Moreover, Fig. 7 reveals that the artefact waveforms depicted in Fig. 6a, averaged at each echo-planar imaging slice time, are quite similar to the artefact templates estimated by the established AAS methodology (Allen et al., 2000; Ferreira et al., 2013). The average cross-correlation calculated between these average artefact waveforms is equal to

0.996 as well. This fact demonstrates that the artefact variability over the time is predicted by the sum-of-sinusoid models (Ferreira et al., 2013).

Therefore, such features allow the usage of the proposed sum-of-sinusoids modelling approach for an effective representation and extraction of frequency components in ECG signals and gradient artefacts in EEG signals. In future work, such a method shall be applied and assessed for other types of biological signals and other types of artefact.

Conclusions

In this work, we have made use of a filter technique based upon the sum of a set of sinusoidal waveforms to model and extract signal frequency components in physiological signals.

According to our modelling approach, each frequency component is approximated as a sinusoid, whose amplitude and phase are estimated by making use of the Discrete Fourier Transform magnitude and phase parameters.

The proposed methodology shows to achieve an accurate representation of signal components in ECG signals and underlying gradient artefacts in EEG signals. The subtraction of the sum-of-sinusoids model still allows a satisfactory removal of the underlying gradient artefact from the EEG signal. Therefore, such characteristics enable its use as an effective approach for extraction and filtering of frequency components of interest in biological signals.

ACKNOWLEDGMENT

We are grateful to Saskia van Liempt, M. D., and Col. Eric Vermetten, M. D., Ph.D. from the University Medical Center /Central Military Hospital, Utrecht, for providing the data presented in this work. This work has been made possible by a grant from the European Union and Erasmus Mundus – EBW II Project, and by a grant from CNPq – Science without Borders Program.

REFERENCES

Allen, P., Polizzi, G., Krakow, K., Fish, D., Lemieux, L. "Identification of EEG events in the MR scanner: the problem of pulse artefact and a method for its subtraction." NeuroImage8 (1998): 229-239.

Allen, P., Josephs, O., Turner, R. "A method for removing imaging artifact from continuous EEG recorded during functional MRI." NeuroImage 12 (2000): 230-239.

Brillinger, D. "Fitting cosines: Some procedures and some physical examples." In Applied probability, stochastic process and sampling theory, edited by I.MacNeill and J. Umphrey, 75–100. Dordrecht: Reidel, 1987.

El-Tatar, A., Fokapu, O."Modeling MR induced artifacts contaminating electrophysiological signals recorded during MRI." 33rd Annual International Conference of the IEEE EMBS, Boston, Massachusetts, August 30 – September 3, 2011, Proceedings: 7135-7138, 2011.

Ferreira, J., Cluitmans, P., Aarts, R.M. "Gradient artefact correction in the EEG signal recorded within the fMRI scanner." 5th International Conference on Bio-inspired Systems and Signal Processing, BIOSIGNALS 2012, Vilamoura, Portugal, February 1-4, 2012, Proceedings: 110-117, 2012.

Ferreira, J., Cluitmans, P., Aarts, R.M. "Gradient artefact modelling using a set of sinusoidal waveforms for EEG correction during continuous fMRI." Signal Processing Research 2 (2013): 39-48.

Goodwin, M. "The STFT, sinusoidal models, and speech modification." In Spring handbook of speech processing, edited by J. Benesty, M. Sondhi, Y. Huang, 229-256. New York: Springer, 2008.

Kay, S. Fundamentals of statistical signal processing: estimation theory. Upper Saddle River: Prentice Hall, 1993.

Koskinen, M., Vartiainen, N. "Removal of imaging artifacts in EEG during simultaneous EEG/fMRI recording: reconstruction of a high-precision artifact template." NeuroImage 46 (2009): 160-167.

McAulay, R., Quatieri, T. "Speech analysis/synthesis based on a sinusoidal representation." IEEE Transactions on Acoustics, Speech, and Signal Processing 34 (1986): 744-754.

Niazy, R., Beckmann, C., Iannetti, G., Brady, J., Smith, S. "Removal of FMRI environment artifacts from EEG data using optimal basis sets." NeuroImage 28 (2005): 720-737.

Olson, W. "Basic concepts of medical instrumentation." In Medical instrumentation: application and design, edited by J. Webster, 1-44. 4thed. New York: Wiley, 2010.

Oppenheim, A., Schafer, R. Discrete-Time Signal Processing. 2thed. New Jersey: Prentice-Hall, 1999.

Papoulis, A.; Pillai, S. Probability, random variables, and

stochastic processes. 4thed. New York: McGraw-Hill, 2002.

Prasad, A., Kundu, D., Mitra, A. "Sequential estimation of the sum of sinusoidal model parameters." J. Statist. Plann. Inference 138 (2008): 1297-1313.

Proakis, J., Manolakis, D. Digital Signal Processing: principles, algorithms and applications. 3rded. New Jersey: Prentice-Hall, 1996.

Rangayyan, R. Biomedical signal analysis: a case-study approach. New York: Wiley, 2002.

Van Liempt, S., Vermetten, E., Lentjes, E., Arends, J., Westenberg, H. "Decreased nocturnal growth hormone secretion and sleep fragmentation in combat-related posttraumatic stress disorder; potential predictors of impaired memory consolidation." Psychoneuroendocrino 36 (2011): 1361-1369.

Vaseghi, S. Advanced digital signal processing and noise reduction.2thed. New York: Wiley, 2000.